

Efficient simulation of railway pantograph/ catenary interaction using pantograph-fixed coordinates

Daniel Ritzberger* Emir Talic* Alexander Schirrer*

* Vienna University of Technology, Austria, (e-mail:
daniel.ritzberger@gmail.com).

Abstract: In this paper, a novel approach for the simulation of the railway catenary and pantograph dynamics is proposed. The partial differential equations describing the vertical motion of the contact and carrier wires of the catenary are transformed in such a way that the pantograph is at rest with respect to the new moving coordinate. The computational domain is then truncated and absorbing boundary conditions are applied. High computational performance due to a great reduction in variables is achieved. The differences between this small scale system and a reference system with a fixed catenary length and a moving pantograph are investigated.

© 2015, IFAC (International Federation of Automatic Control) Hosting by Elsevier Ltd. All rights reserved.

Keywords: Modelling Aspects in Scientific Computing; Numerical and Symbolical Methods for Modelling

1. INTRODUCTION

A numerical simulation of the complex catenary and pantograph dynamics (see Fig. 1) can give a better insight on how they interact with one another and lead to better design rules for the pantograph to prevent contact loss and electric arcing. The dynamics are described by coupled partial differential equations (PDEs). The classic approach for modelling the pantograph and catenary interaction, see Arnold and Simeon (2000) and Poetsch et al. (1997), is with respect to a resting catenary and a moving pantograph. This formulation is also predominant in many recent papers studying more complex phenomena like wind disturbances and co-simulation of multi-body pantograph models, see Pombo et al. (2009). For real-time applications a simplified mathematical model of the catenary can be obtained by using the modal superposition principle (Facchinetti and Bruni (2012), Zhang et al. (2002)). In the resting catenary formulation, the maximal simulation time is limited by the length of the catenary. Longer simulations consequently increase the number of variables of the dynamical system and the computational effort. Also if the pantograph is currently moving near the boundary, reflections occur. These unphysical reflections decrease the quality of the simulation and directly disturb the pantograph-catenary-interaction. A new approach that deals with these problems is presented here.

In this work a new formulation for the problem is introduced with the goal to make the size of the computational domain independent from the simulation time, and reducing the computational effort, so that the simulation can be carried out in real-time. This is achieved by a transformation of the PDEs, which describe the catenary dynamics, to moving coordinates. The pantograph is now at a fixed location with respect to the new coordinate and the catenary moves over the pantograph through the computational domain. To eliminate the disturbances

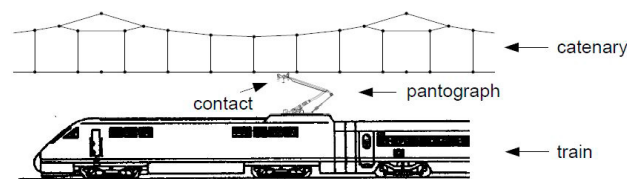


Fig. 1. System Catenary/ Pantograph, taken from Poetsch et al. (1997)

due to reflections at the boundaries, absorbing boundary conditions (ABCs) are introduced which ideally let waves leave the computational domain without reflections. Thus, the length of this system can be chosen reasonably small, reducing the number of variables to be calculated. Using the transformed equations with a fixed pantograph an "endless" catenary is approximated on a bounded computational domain.

The structure of this paper is as follows: In chapter 2, the methodology used for the novel system formulation is discussed. In chapter 3, a concrete numerical system is assembled, and in chapter 4, the small-scale moving system and a large reference system with fixed catenary and moving pantograph are compared in numerical results.

2. METHODOLOGY

In this chapter, the equation of motion for a pretensioned Euler-Bernoulli-Beam equation, its transformation to a moving coordinate, a simple ABC formulation and its discretization are discussed.

2.1 Transforming the Equations of Motion

The transversal motion of the contact and carrier wire is described by a pretensioned Euler-Bernoulli-Beam equation.

$$\rho A \frac{\partial^2 w(x, t)}{\partial t^2} + \beta \frac{\partial w(x, t)}{\partial t} = -EI \frac{\partial^4 w(x, t)}{\partial x^4} + T \frac{\partial^2 w(x, t)}{\partial x^2} + f(x, t) \quad (1)$$

Thereby, ρA is the mass per unit length, β the damping constant, EI the bending stiffness, T the tensile axial force and $f(x, t)$ is the vertical force density. Equation (1) is transformed using a new coordinate $\hat{x}(t) = x + vt$ where v is the constant pantograph speed. Because $\frac{\partial \hat{x}}{\partial x} = 1$, the spatial partial derivatives, $\frac{\partial^n w(x(t), t)}{\partial x^n} = \frac{\partial^n w(\hat{x}(t), t)}{\partial \hat{x}^n}$, remains simple. The new coordinate is time-dependent, which has to be considered for the partial derivative with respect to t . Using implicit differentiation one obtains

$$\frac{dw(\hat{x}(t), t)}{dt} = \frac{\partial w(\hat{x}, t)}{\partial t} - v \frac{\partial w(\hat{x}, t)}{\partial \hat{x}} \quad (2)$$

and

$$\frac{d^2 w(\hat{x}(t), t)}{dt^2} = \frac{\partial^2 w(\hat{x}, t)}{\partial t^2} - 2v \frac{\partial^2 w(\hat{x}, t)}{\partial \hat{x} \partial t} + v^2 \frac{\partial^2 w(\hat{x}, t)}{\partial \hat{x}^2} \quad (3)$$

Inserting (2) and (3) into (1) leads to the following equation of motion for a pretensioned Euler-Bernoulli beam with respect to a moving spatial coordinate.

$$\rho A \ddot{w} + \beta \dot{w} = -EI w'''' + (T - \rho A v^2) w'' + \beta v w' + 2v \rho A \dot{w}' + f(\hat{x}, t) \quad (4)$$

To keep the notation simple the abbreviations $\frac{\partial w}{\partial t} = \dot{w}$ and $\frac{\partial w}{\partial \hat{x}} = w'$ are used, with higher order of derivatives respectively. Note that the transformed equation of motion now contains the mixed derivative \dot{w}' .

2.2 Absorbing Boundary Conditions

ABCs are used to minimize the reflections of waves at the computational boundary. For a detailed discussion of the ABCs see Engquist and Majda (1977) or Higdon (1987). The first order approximation of the perfect absorbing boundary condition is used, which is exact for the one-dimensional wave equation:

$$\dot{w} \pm (c \mp v) w' = 0, \quad (5)$$

$$c = \sqrt{\frac{T}{\rho A}},$$

where c is the wave speed. Eq. (5) has to be fulfilled at the boundary. The signs of the second term differs for the left and for the right boundary, as there are left- and right-going waves to be absorbed, and the wave speed for left going waves is increased by v while the wave speed for right going waves is decreased by v .

A stable discretization of Eq. (5) is obtained by using a forward difference approximation for the partial derivative

with respect to time. The spatial partial derivative is discretized by forward differences for the left boundary and backward differences for the right boundary. This leads to the discrete ABC for the left boundary

$$w_1^{j+1} = (1 - (c + v) \frac{\Delta t}{\Delta x}) w_1^j + (c + v) \frac{\Delta t}{\Delta x} w_2^j \quad (6)$$

and for the right boundary

$$w_{n_{max}}^{j+1} = (1 - (c - v) \frac{\Delta t}{\Delta x}) w_{n_{max}}^j + (c - v) \frac{\Delta t}{\Delta x} w_{n_{max}-1}^j \quad (7)$$

The discrete ABCs are only exact for the scalar wave equation and if

$$\frac{\Delta t}{\Delta x} = \frac{1}{c} \quad (8)$$

Since Eq. (6) and (7) are imposed on the pretensioned Euler-Bernoulli-beam and the ratio for the spatial and temporal grid size (8) cannot be set to c because of stability issues, the ABCs are not exact and reflections occur. Using the scalar wave ABCs is the first approach on introducing reflectionless boundaries for the pretensioned Euler-Bernoulli beam. In future work, a genetically optimized boundary stencil for the moving Euler-Bernoulli beam will be used, see Schirrer et al. (2014)

3. SYSTEM ASSEMBLY

Using the methodology discussed above, a dynamic formulation of the catenary/ pantograph interaction and its discretization is obtained.

3.1 Description

As it can be seen in Fig. 2, the catenary consists of two wires, the carrier and the contact wire. The contact wire is suspended by droppers from the carrier wire in such a way that the static displacement of the contact wire is minimized. The head of the pantograph pushes against the contact wire.

For the contact and the carrier wire, the transformed Euler-Bernoulli beam equation (4)

$$\rho_c A_c \ddot{w}_c + \beta_c \dot{w}_c = -E_c I_c w_c'''' + (T_c - \rho_c A_c v^2) w_c'' + \beta_c v w_c' + 2\rho_c A_c v \dot{w}_c' + f_c(\hat{x}, t) \quad (9)$$

$$\rho_w A_w \ddot{w}_w + \beta_w \dot{w}_w = -E_w I_w w_w'''' + (T_w - \rho_w A_w v^2) w_w'' + \beta_w v w_w' + 2\rho_w A_w v \dot{w}_w' + f_w(\hat{x}, t) \quad (10)$$

is used.

The subscript w denotes the displacement and parameters for the contact wire and c the displacement and parameters for the carrier wire.

The pantograph is modelled as a two-mass oscillator. Its equations of motion are given by

$$\begin{aligned} m_1 w_{p,1} &= -d_1 (\dot{w}_{p,1} - \dot{w}_{p,2}) - c_1 (w_{p,1} - w_{p,2}) - F_{cont} \\ m_2 w_{p,2} &= -d_2 \dot{w}_{p,2} + d_1 (\dot{w}_{p,1} - \dot{w}_{p,2}) - c_2 w_{p,2} + \\ &\quad c_1 (w_{p,1} - w_{p,2}) + F_0 \end{aligned} \quad (11)$$

Download English Version:

<https://daneshyari.com/en/article/713551>

Download Persian Version:

<https://daneshyari.com/article/713551>

[Daneshyari.com](https://daneshyari.com)